1997

Introduction to the Bethe Ansatz I

Michael Karbach
University of Rhode Island

Gerhard Müller
University of Rhode Island, gmuller@uri.edu

Citation/Publisher Attribution
M. Karbach and G. Müller. Introduction to the Bethe ansatz I. Computers in Physics 11 (1997), 36-43.
Available at: http://dx.doi.org/10.1063/1.4822511

Introduction to the Bethe Ansatz I

Michael Karbach* and Gerhard Müller†
*Bergische Universität Wuppertal, Fachbereich Physik, D-42097 Wuppertal, Germany
†Department of Physics, University of Rhode Island, Kingston RI 02881-0817
(February 1, 2008)

A few years after the formulation of quantum mechanics, Heisenberg and Dirac[1] discovered that one of its wondrous consequences was the key to the age-old mystery of ferromagnetism. They found that the laws of quantum mechanics imply the existence of an effective interaction, $J_{ij}\,\mathbf{S}_i\cdot\mathbf{S}_j$, between electron spins on neighboring atoms with overlapping orbital wave functions. The exchange interaction, as it has become known, is caused by the combined effect of the Coulomb repulsion and the Pauli exclusion principle. This spin interaction was soon recognized to be the key to a microscopic theory of ferromagnetism and many other cooperative phenomena involving electron spins.

In 1931 Hans Bethe[2] presented a method for obtaining the exact eigenvalues and eigenvectors of the one-dimensional (1D) spin-1/2 Heisenberg model, a linear array of electrons with uniform exchange interaction between nearest neighbors. Bethe's parametrization of the eigenvectors, the *Bethe ansatz*, has become influential to an extent not imagined at the time. Today, many other quantum many body systems are known to be solvable by some variant of the Bethe ansatz, and the method has been generalized and expanded far beyond the ad hoc calculational tool it was originally. Unlike the simulation of a classical model system, most computational approaches to quantum many-body systems require a fair amount of analytical work up front. This requirement is true for Monte Carlo calculations, renormalization group approaches, the recursion method, large-scale numerical diagonalizations, and for the Bethe ansatz when used in a computational context.

In spite of its proven importance and wide range of applications, the Bethe ansatz is rarely discussed in textbooks on quantum mechanics and statistical mechanics except at the advanced level. The goal of this column is to introduce the Bethe ansatz at an elementary level. In future columns we plan to discuss some of the extensions, generalizations, and applications of the method, to which many workers have made important contributions. Our emphasis will be on computational applications for which the method is less well known than for its usefulness as an analytical tool.

The Bethe ansatz is an exact method for the calculation of eigenvalues and eigenvectors of a limited but select class of quantum many-body model systems. Although the eigenvalues and eigenvectors for a finite system may be obtained with less effort from a brute force numerical diagonalization, the Bethe ansatz offers two important advantages: (i) all eigenstates are characterized by a set of quantum numbers which can be used to distinguish them according to specific physical properties; (ii) in many cases the eigenvalues and the physical properties derived from them can be evaluated in the thermodynamic limit.

The Hamiltonian of the Heisenberg model of spins $\mathbf{S}_n=(S_n^x,S_n^y,S_n^z)$ with quantum number $s=1/2$ on a 1D lattice of N sites with periodic boundary conditions $\mathbf{S}_{N+1}=\mathbf{S}_1$ is given by

$$H=-J\sum_{n=1}^{N}\mathbf{S}_n\cdot\mathbf{S}_{n+1}$$
$$=-J\sum_{n=1}^{N}\left[\frac{1}{2}\big(S_n^+S_{n+1}^-+S_n^-S_{n+1}^+\big)+S_n^zS_{n+1}^z\right],\qquad(1)$$

where $S_n^\pm\equiv S_n^x\pm iS_n^y$ are spin flip operators. H acts on a Hilbert space of dimension 2^N spanned by the orthogonal basis vectors $|\sigma_1\ldots\sigma_N\rangle$, where $\sigma_n=\uparrow$ represents an up spin and $\sigma_n=\downarrow$ a down spin at site n. The spin commutation relations (with $\hbar=1$) are

$$[S_n^z,S_{n'}^\pm]=\pm S_n^\pm\delta_{nn'},\quad [S_n^+,S_{n'}^-]=2S_n^z\delta_{nn'}.\qquad(2)$$

The application of the operators $S_n^\pm,S_n^z$ on a vector $|\sigma_1\ldots\sigma_N\rangle$ yields the results summarized in Table I. We can use these rules to express H as a real and symmetric $2^N\times 2^N$ matrix whose eigenvectors can be computed by standard diagonalization algorithms[3]. From the eigenvectors, the physical quantities of interest can be calculated by evaluating the expectation values (matrix elements) for the corresponding operators.

TABLE I. Rules governing the application of the spin operators on the basis vectors $|\sigma_1\ldots\sigma_N\rangle$ with $\sigma_n=\uparrow,\downarrow$.

	$\vert\ldots\uparrow\ldots\rangle$	$\vert\ldots\downarrow\ldots\rangle$
S_k^+	0	$\vert\ldots\uparrow\ldots\rangle$
S_k^-	$\vert\ldots\downarrow\ldots\rangle$	0
S_k^z	$\frac{1}{2}\vert\ldots\uparrow\ldots\rangle$	$-\frac{1}{2}\vert\ldots\downarrow\ldots\rangle$

The Hamiltonian matrix can be written in block diagonal form if we perform, prior to the numerical diagonalization, one or several basis transformations from $\{|\sigma_1\ldots\sigma_N\rangle\}$ to a symmetry-adapted basis. These transformations reduce the computational effort needed for the remaining numerical diagonalization and make it possible to handle larger system sizes.

The Bethe ansatz is a basis transformation that does not have to be supplemented by a numerical diagonalization. In principle and usually in practice, this alternative

procedure removes the cap on system sizes. However, the implementation of the Bethe ansatz entails calculational challenges of its own. Depending on the specifics of the application, they can be met by analytical or computational methods as we shall see in the following.

For the Heisenberg model, two symmetries are essential for the application of the Bethe ansatz. The rotational symmetry about the z-axis in spin space, which we have chosen to be the quantization axis, implies that the z-component of the total spin $S_T^z \equiv \sum_{n=1}^N S_n^z$ is conserved: $[H, S_T^z] = 0$. According to the rules of Table I, the operation of H on $|\sigma_1 \dots \sigma_N\rangle$ yields a linear combination of basis vectors, each of which has the same number of down spins. Hence, sorting the basis vectors according to the quantum number $S_T^z = N/2 - r$, where r is the number of down spins, is all that is required to block diagonalize the Hamiltonian matrix.

The block with $r = 0$ (all spins up) consists of a single vector $|F\rangle \equiv |\uparrow \dots \uparrow\rangle$. It is an eigenstate, $H|F\rangle = E_0|F\rangle$, with energy $E_0 = -JN/4$. The N basis vectors in the invariant subspace with $r = 1$ (one down spin) are labeled by the position of the flipped spin:

$$|n\rangle = S_n^-|F\rangle \qquad n = 1, \dots, N. \tag{3}$$

To diagonalize the $r = 1$ block of H, which has size $N \times N$, we take into account the translational symmetry, i.e., the invariance of H with respect to discrete translations by any number of lattice spacings. Translationally invariant basis vectors can be constructed from the vectors in (3) by writing

$$|\psi\rangle = \frac{1}{\sqrt{N}} \sum_{n=1}^{N} e^{ikn}|n\rangle \tag{4}$$

for wave numbers $k = 2\pi m/N$, $m = 0, \dots, N-1$. (The lattice spacing has been set equal to unity.) The vectors $|\psi\rangle$ are eigenvectors of the translation operator with eigenvalues e^{ik} and are also eigenvectors of H with eigenvalues

$$E - E_0 = J(1 - \cos k), \tag{5}$$

as can be verified by inspection (see Problem 1). The vectors (4) represent magnon excitations, in which the complete spin alignment of the ferromagnetic ground state $|F\rangle$ is periodically disturbed by a spin wave with wavelength $\lambda = 2\pi/k$ (see Problem 2).

In the invariant subspaces with $2 \le r \le N/2$, the translationally invariant basis does not completely diagonalize the Hamiltonian matrix even if we take into account further symmetries of (1) such as the full rotational symmetry in spin space or the reflection symmetry on the lattice. Here the Bethe ansatz is a powerful alternative.

For $r = 1$, the case we have already solved, we now proceed somewhat differently. Any eigenvector in the $r = 1$ subspace is a superposition of the basis vectors (3):

$$|\psi\rangle = \sum_{n=1}^{N} a(n)|n\rangle. \tag{6}$$

The eigenvector $|\psi\rangle$ is a solution of the eigenvalue equation $H|\psi\rangle = E|\psi\rangle$ if the coefficients $a(n)$ satisfy the linear equations

$$2[E - E_0]a(n) = J[2a(n) - a(n-1) - a(n+1)] \tag{7}$$

for $n = 1, 2, \dots, N$ and with periodic boundary conditions $a(n+N) = a(n)$. N linearly independent solutions of (7) are

$$a(n) = e^{ikn}, \qquad k = \frac{2\pi}{N}m, \qquad m = 0, 1, \dots, N-1. \tag{8}$$

If we substitute the coefficients $a(n)$ into (6), we obtain (after normalization) the magnon states (4) with energies (5).

The distinctive features of the Bethe ansatz begin to emerge when we apply the same procedure to the case $r = 2$. The task is to determine the coefficients $a(n_1, n_2)$ for all eigenstates

$$|\psi\rangle = \sum_{1 \le n_1 < n_2 \le N} a(n_1, n_2)|n_1, n_2\rangle, \tag{9}$$

where $|n_1, n_2\rangle \equiv S_{n_1}^- S_{n_2}^-|F\rangle$ are the basis vectors in this subspace of dimension $N(N-1)/2$. Bethe's preliminary ansatz for the coefficients is

$$a(n_1, n_2) = Ae^{i(k_1 n_1 + k_2 n_2)} + A'e^{i(k_1 n_2 + k_2 n_1)}. \tag{10}$$

We might wish to set $A = A'$, use the same values for k_1, k_2 as in (8), and interpret the wave function as a superposition of two magnons. However, the result would be an overcomplete set of $N(N+1)/2$ nonorthogonal and nonstationary states. Superimposed spin waves are in conflict with the requirement that the two flipped spins must be at different sites. The eigenvalue equation for (9) translates into $N(N-1)/2$ equations for as many coefficients $a(n_1, n_2)$:

$$\begin{aligned} 2[E - E_0]a(n_1, n_2) = J[&4a(n_1, n_2) - a(n_1 - 1, n_2) \\ &- a(n_1 + 1, n_2) - a(n_1, n_2 - 1) - a(n_1, n_2 + 1)] \\ &\text{for} \quad n_2 > n_1 + 1, \end{aligned} \tag{11a}$$

$$\begin{aligned} 2[E - E_0]a(n_1, n_2) = J[&2a(n_1, n_2) - a(n_1 - 1, n_2) \\ &- a(n_1, n_2 + 1)] \\ &\text{for} \quad n_2 = n_1 + 1. \end{aligned} \tag{11b}$$

Equations (11a) are satisfied by $a(n_1, n_2)$ in (10) with arbitrary A, A', k_1, k_2 for $n_2 > n_1 + 1$ and for $n_2 = n_1 + 1$ provided the energy depends on k_1, k_2 as follows:

$$E - E_0 = J \sum_{j=1,2} (1 - \cos k_j). \tag{12}$$

Equations (11b), which are not automatically satisfied by the ansatz (10), are then equivalent to the N conditions

$$2a(n_1, n_1+1) = a(n_1, n_1) + a(n_1+1, n_1+1) \qquad (13)$$

obtained by subtracting (11b) from (11a) for $n_2 = n_1+1$. In other words, $a(n_1, n_2)$ are solutions of Eqs. (11) if they have the form (10) and satisfy (13). The conditions (13) require a modification of the amplitude ratio,

$$\frac{A}{A'} \equiv e^{i\theta} = -\frac{e^{i(k_1+k_2)} + 1 - 2e^{ik_1}}{e^{i(k_1+k_2)} + 1 - 2e^{ik_2}}. \qquad (14)$$

This requirement is incorporated into the Bethe ansatz as extra phase factors

$$a(n_1, n_2) = e^{i(k_1 n_1 + k_2 n_2 + \frac{1}{2}\theta_{12})} + e^{i(k_1 n_2 + k_2 n_1 + \frac{1}{2}\theta_{21})}, \quad (15)$$

where the phase angle $\theta_{12} = -\theta_{21} \equiv \theta$ depends on the as yet undetermined k_1, k_2 via (14) or, in real form, via

$$2\cot\frac{\theta}{2} = \cot\frac{k_1}{2} - \cot\frac{k_2}{2}. \qquad (16)$$

The quantities k_1, k_2 will henceforth be referred to as momenta of the Bethe ansatz wave function (9) with coefficients (15).

Two additional relations between k_1, k_2, and θ follow from the requirement that the wave function (9) be translationally invariant, which implies that $a(n_1, n_2) = a(n_2, n_1 + N)$. This condition is satisfied by the coefficients (15) if $e^{ik_1 N} = e^{i\theta}$, $e^{ik_2 N} = e^{-i\theta}$. Equivalently, we can write (after taking logarithms)

$$Nk_1 = 2\pi\lambda_1 + \theta, \qquad Nk_2 = 2\pi\lambda_2 - \theta, \qquad (17)$$

where the integers $\lambda_i \in \{0, 1, \ldots, N-1\}$ are called Bethe quantum numbers.

The remaining task is to find all (λ_1, λ_2) pairs which yield solutions of Eqs. (16) and (17), known as the Bethe ansatz equations. Every eigenstate in the $r = 2$ subspace can be found in this way. For any solution k_1, k_2, θ, the (non-normalized) eigenvector has coefficients of the form (15). The expression (12) for the energy and the relation

$$k = k_1 + k_2 = \frac{2\pi}{N}(\lambda_1 + \lambda_2) \qquad (18)$$

for the wave number k are reminiscent of two superimposed magnons. The magnon interaction is reflected in the phase shift θ and in the deviation of the momenta k_1, k_2 from the values of the one-magnon wave numbers as given in (8). We shall see that the magnons either scatter off each other or form bound states. Note that the momenta k_1, k_2 specify the Bethe ansatz wave function (9), while the wave number k is the quantum number associated with the translational symmetry of H and exists independently of the Bethe ansatz.

The analysis of the complete $r = 2$ spectrum will demonstrate the usefulness of the Bethe quantum numbers for distinguishing eigenstates with different physical properties. The allowed (λ_1, λ_2) pairs are restricted to $0 \le \lambda_1 \le \lambda_2 \le N-1$. Switching λ_1 and λ_2 simply interchanges k_1 and k_2 and produces the same solution. There are $N(N+1)/2$ pairs that meet this restriction, but only $N(N-1)/2$ of them yield a solution of Eqs. (16) and (17). The solutions can be determined analytically or computationally. Some of them have real k_1, k_2, and others yield complex conjugate momenta, $k_2 = k_1^*$.

We first find all the solutions and then interpret them. The (λ_1, λ_2) pairs which yield solutions for $N = 32$ are shown in Fig. 1. We begin with the class C_1 of states

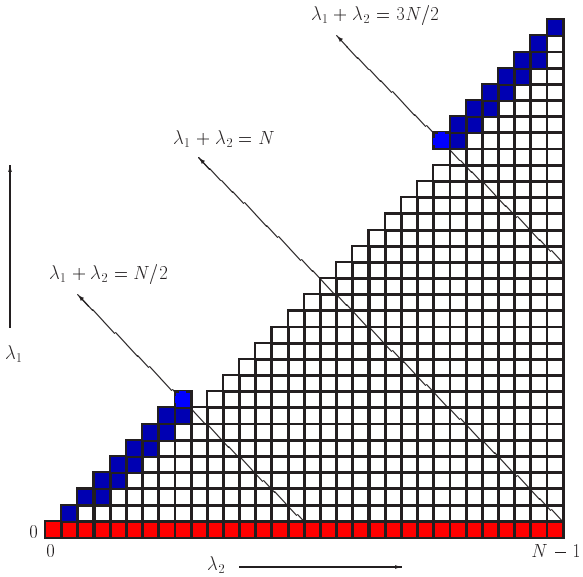

FIG. 1. The allowed pairs of Bethe quantum numbers (λ_1, λ_2) that characterize the $N(N-1)/2$ eigenstates in the $r = 2$ subspace for $N = 32$. The states of class C_1, C_2, and C_3 are colored red, white, and blue, respectively.

for which one of the Bethe quantum numbers is zero, $\lambda_1 = 0, \lambda_2 = 0, 1, \ldots, N-1$. There exists a real solution for all N combinations, $k_1 = 0, k_2 = 2\pi\lambda_2/N, \theta = 0$ (see Problem 3).

Next consider the class C_2 of states with nonzero λ_1, λ_2 which differ by two or more: $\lambda_2 - \lambda_1 \ge 2$. There are $N(N-5)/2 + 3$ such pairs. All of them yield a solution with real k_1, k_2. To determine these solutions, we combine Eqs. (16), (17), and (18) into a single nonlinear equation for k_1:

$$2\cot\frac{Nk_1}{2} = \cot\frac{k_1}{2} - \cot\frac{k - k_1}{2}. \qquad (19)$$

The solution k_1 of (19) for a given wave number $k = (2\pi n/N)$, $n = 0, 1, \ldots, N-1$ is substituted into (17) and yields k_2 and θ. Some of the solutions can be found

analytically (Problem 4), and others must be determined numerically (Problem 5).

The remaining class C_3 of states has nonzero Bethe quantum numbers λ_1, λ_2 which either are equal or differ by unity. There exist $2N-3$ such pairs, but we will see that only $N-3$ pairs yield solutions of (16) and (17). Most of the class C_3 solutions are complex. To find them, we write

$$k_1 \equiv \frac{k}{2} + iv, \quad k_2 \equiv \frac{k}{2} - iv, \quad \theta \equiv \phi + i\chi, \tag{20}$$

and use Eqs. (16) and (17) for fixed k to obtain the relation

$$\cos\frac{k}{2}\sinh(Nv) = \sinh[(N-1)v] + \cos\phi\sinh v, \tag{21}$$

where $\phi = \pi(\lambda_1 - \lambda_2)$, and $\chi = Nv$ is inferred from the solution. It is sufficient to consider $v > 0$. The energy (12) of any complex solution is rewritten in the form

$$E - E_0 = 2J\left(1 - \cos\frac{k}{2}\cosh v\right). \tag{22}$$

Inspection of (21) shows (see Problem 6) that a complex solution exists for $\lambda_2 = \lambda_1$ if

$$\lambda_1+\lambda_2 = 2, 4, \ldots, \frac{N}{2}-2, \frac{3N}{2}+2, \ldots, 2N-2. \tag{23}$$

For $\lambda_2 = \lambda_1 + 1$ a complex solution exists if

$$\lambda_1+\lambda_2 = \tilde{\lambda}, \tilde{\lambda}+2, \ldots, N/2-1, 3N/2+3, \ldots, 2N-\tilde{\lambda}+2, \tag{24}$$

where $\tilde{\lambda} \approx \sqrt{N}/\pi$. In the latter case, there exist additional real solutions of (19) if

$$\lambda_1 + \lambda_2 = 3, 5, \ldots, \tilde{\lambda}-2, 2N-\tilde{\lambda}+2, \ldots, 2N-3. \tag{25}$$

The (λ_1, λ_2) pairs in (23)–(25) account for $N-4$ solutions in class C_3. There is one more class C_3 solution. This state, which has $k = \pi$ and $\lambda_1 = \lambda_2 = N/4$, is easily missed in the numerical analysis, because k_1, k_2 have an infinite imaginary part (see Problem 7).

The complete $r = 2$ excitation spectrum $(E - E_0)/J$ versus k for a system with $N = 32$ spins as obtained by the analytical and computational procedures outlined in Problems 3–7 is plotted in Fig. 2. The N states of class C_1 form a branch with exactly the same dispersion relation (5) as the magnon states that populate the $r = 1$ subspace. This degeneracy is a consequence of the conservation of the total spin S_T (see Problem 8). The class C_2 states are spread in a regular pattern over a region in (k, E)-space. They are nearly free superpositions of two one-magnon states.

The excitations belonging to classes C_1 and C_2 can be characterized as two-magnon scattering states. The

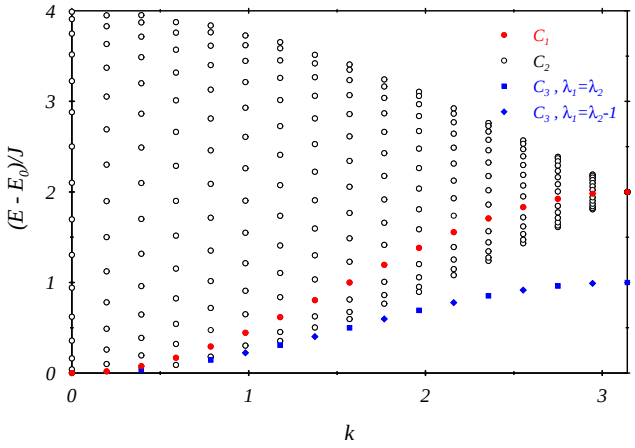

FIG. 2. Excitation energy $(E - E_0)/J$ versus wave number k of all $N(N-1)/2$ eigenstates in the invariant subspace with $r = 2$ overturned spins for a system with $N = 32$. States of class C_1 are denoted by red circles, states of class C_2 by open black circles, and states of class C_3 by blue squares if $\lambda_2 = \lambda_1$, or blue diamonds if $\lambda_2 = \lambda_1 + 1$.

effect of the magnon interaction on these states is visualized in Fig. 3. It shows all $N(N-1)/2 - N + 3$ class C_1 and class C_2 states for $N = 32$ in comparison with the $N(N+1)/2$ two-magnon superpositions, where the momenta $k_j, j = 1, 2$ in (12) are replaced by one-magnon wave numbers $k_j = 2\pi m_j/N$, $m_j = 0, 1, \ldots, N-1$. The magnon interaction manifests itself as a modified excitation energy of the two-magnon scattering states. Note that the interaction energy approaches zero when either k_1 or k_2 goes to zero. The class C_1 states can then be interpreted as exact superpositions of a $k_1 = 0$ magnon and a $k_2 \neq 0$ magnon.

As N increases, the energy correction due to the magnon interaction diminishes for the class C_2 states as well and vanishes in the limit $N \to \infty$. The two-magnon scattering states then form a continuum with boundaries $E - E_0 = 2J(1 \pm \cos k/2)$, which coincide with those of the continuum of free two-magnon states.

For the class C_3 states, the effects of the magnon interaction are much more prominent, and they do not disappear in the limit $N \to \infty$. In the (k, E)-plane of Fig. 2, these states lie on a single branch with dispersion (see Problem 9)

$$E - E_0 = \frac{J}{2}(1 - \cos k) \tag{26}$$

below the continuum of two-magnon scattering states. They are the two-magnon bound states.

The bound state character of the class C_3 states manifests itself in the enhanced probability that the two flipped spins are on neighboring sites of the lattice. This property of the wave function is best captured in the weight distribution $|a(n_1, n_2)|$ of basis vectors with

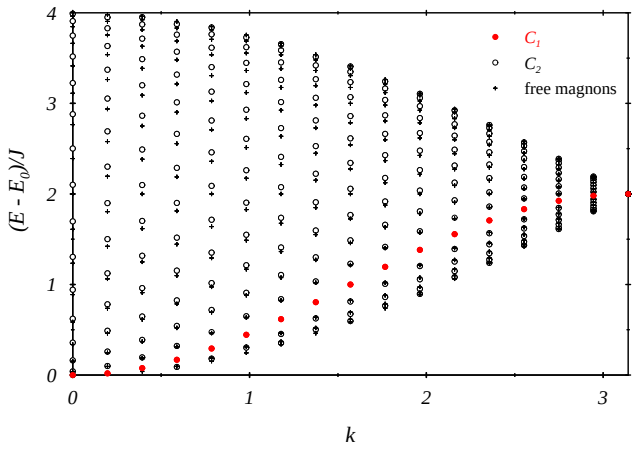

FIG. 3. Excitation energy $(E-E_0)/J$ versus wave number k of all two-magnon scattering states (classes C_1 and C_2 from Fig. 2) for a system with $N = 32$ in comparison with the noninteracting magnon pairs (+).

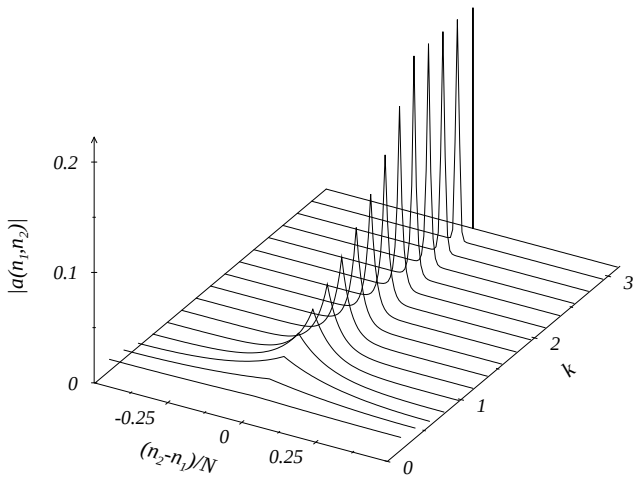

FIG. 4. Weight distribution $|a(n_1,n_2)|$ versus distance n_2-n_1 of the two down spins of class C_3 states at $k=(2\pi/N)n,\ n=4,8,\ldots,N/2$ for $N=128$.

flipped spins at sites n_1 and n_2. In Fig. 4 we plot $|a(n_1,n_2)|$ versus n_2-n_1 for a sequence of class C_3 states between $k=0$ and $k=\pi$. The distribution is peaked at $n_2-n_1=1$. Its width is controlled by the imaginary parts of k_1,k_2,θ in the coefficients (15). The smallest width is observed in the bound state at $k=\pi$, that is, for $\lambda_1=\lambda_2=N/4$, whose k_1,k_2 have an infinite imaginary part (see Problem 7). In this case, all coefficients in (9) with $n_2\neq n_1+1$ are zero, which implies that the two down spins are tightly bound together and have the largest binding energy. For the adjacent bound state with quantum numbers $\lambda_1=\lambda_2=N/4-1$, the exponential dependence of the weight $|a(n_1,n_2)|$ on the separation n_2-n_1 can be worked out analytically (see Problem 9).

The width of the distribution $|a(n_1,n_2)|$ increases as k decreases, and the binding of the two down spins loosens. For finite N, the exponential factors disappear when the distribution has acquired a certain width, and the Bethe ansatz solutions switch from complex to real. In contrast, the distribution $|a(n_1,n_2)|$ for scattering states is always broad and oscillates wildly in general. However, for some combinations of k_1,k_2, a smooth distribution ensues, which has its maximum when the two down spins are farthest apart ($n_2=n_1+N/2$) (see Problem 10).

The formation of bound states and scattering states of specific elementary excitations exist in a large variety of physical contexts. But only in rare cases such as this one can the nature and the properties of such compound excitations be investigated (analytically and computationally) on the level of detail made possible by the Bethe ansatz.

We now present the Bethe ansatz for an unrestricted number r of overturned spins. We generalize (9) and expand the eigenstates in the form

$$|\psi\rangle=\sum_{1\le n_1<\ldots<n_r\le N}a(n_1,\ldots,n_r)|n_1,\ldots,n_r\rangle. \tag{27}$$

The subspace has dimension $N!/[(N-r)!r!]$. The generalization of (15) for the coefficients in terms of r momenta k_j, and one phase angle $\theta_{ij}=-\theta_{ji}$ for each (k_1,k_2) pair is as follows:

$$a(n_1,\ldots,n_r)=\sum_{\mathcal{P}\in S_r}\exp\left(i\sum_{j=1}^{r}k_{\mathcal{P}j}n_j+\frac{i}{2}\sum_{i<j}\theta_{\mathcal{P}i\mathcal{P}j}\right). \tag{28}$$

The sum $\mathcal{P}\in S_r$ is over all $r!$ permutations of the labels $\{1,2,\ldots,r\}$. For $r=2$ the two permutations are the identity $(1,2)$ and the transposition $(2,1)$, which produce the two terms of (15). The consistency equations for the coefficients $a(n_1,\ldots,n_r)$ inferred from the eigenvalue equation $H|\psi\rangle=E|\psi\rangle$ are

$$2[E-E_0]a(n_1,\ldots,n_r)=J\sum_{i=1}^{r}\sum_{\sigma=\pm1}[a(n_1,\ldots,n_r) -a(n_1,\ldots,n_i+\sigma,\ldots,n_r)], \tag{29a}$$

for $n_{j+1}>n_j+1,\ j=1,\ldots,r$, and

$$2[E-E_0]a(n_1,\ldots,n_r)= J\sum_{i\neq j_\alpha,j_\alpha+1}^{r}\sum_{\sigma=\pm1}[a(n_1,\ldots,n_r)-a(n_1,\ldots,n_i+\sigma,\ldots,n_r)] +J\sum_{\alpha}[2a(n_1,\ldots,n_r)-a(n_1,\ldots,n_{j_\alpha}-1,n_{j_\alpha+1},\ldots,n_r) -a(n_1,\ldots,n_{j_\alpha},n_{j_\alpha+1}+1,\ldots,n_r)] \tag{29b}$$

for $n_{j_\alpha+1} = n_{j_\alpha} + 1,\ n_{j+1} > n_j + 1,\ j \neq j_\alpha$. The coefficients $a(n_1, \ldots, n_r)$ are solutions of (29) for the energy

$$E - E_0 = J \sum_{j=1}^{r} (1 - \cos k_j) \tag{30}$$

if they have the form (28) and satisfy the conditions

$$2a(n_1, \ldots, n_{j_\alpha}, n_{j_\alpha}+1, \ldots, n_r) = a(n_1, \ldots, n_{j_\alpha}, n_{j_\alpha}, \ldots, n_r) + a(n_1, \ldots, n_{j_\alpha}+1, n_{j_\alpha}+1, \ldots, n_r) \tag{31}$$

for $\alpha = 1, \ldots, r$ just as we have shown for $r = 2$. These conditions relate every phase angle θ_{ij} to the (as yet undetermined) k_j in (27):

$$e^{i\theta_{ij}} = -\frac{e^{i(k_i+k_j)} + 1 - 2e^{ik_i}}{e^{i(k_i+k_j)} + 1 - 2e^{ik_j}}. \tag{32}$$

An equivalent relation in real form reads

$$2 \cot \frac{\theta_{ij}}{2} = \cot \frac{k_i}{2} - \cot \frac{k_j}{2}, \quad i, j = 1, \ldots, r. \tag{33}$$

The translational invariance of (27) implies that the coefficients (28) satisfy the relation $a(n_1, \ldots, n_r) = a(n_2, \ldots, n_r, n_1 + N)$. Consequently, we must have

$$\sum_{j=1}^{r} k_{\mathcal{P}j} n_j + \frac{1}{2} \sum_{i<j} \theta_{\mathcal{P}i, \mathcal{P}j} = \frac{1}{2} \sum_{i<j} \theta_{\mathcal{P}'i, \mathcal{P}'j} - 2\pi \lambda_{\mathcal{P}'r} + \sum_{j=2}^{r} k_{\mathcal{P}'(j-1)} n_j + k_{\mathcal{P}'r}(n_1 + N), \tag{34}$$

where the relation between the permutations on the left and the right is $\mathcal{P}'(i-1) = \mathcal{P}i,\ i = 2, \ldots, r;\ \mathcal{P}'r = \mathcal{P}1$. If we take into account that all terms not involving the index $\mathcal{P}'r = \mathcal{P}1$ cancel, we are left with r additional relations between the phase angles and the momenta:

$$N k_i = 2\pi \lambda_i + \sum_{j \neq i} \theta_{ij}, \quad i = 1, \ldots, r, \tag{35}$$

where $\lambda_i \in \{0, 1, \ldots, N-1\}$ as in (17). What remains to be done is to find those sets of Bethe quantum numbers $(\lambda_1, \ldots, \lambda_r)$ which yield (real or complex) solutions of the Bethe ansatz equations (33) and (35). Every solution represents an eigenvector (27) with energy (30) and wave number

$$k = \frac{2\pi}{N} \sum_{i=1}^{r} \lambda_i. \tag{36}$$

The complete set of Bethe ansatz solutions for systems with $N = 4, 5$, and 6 spins can be read off Tables II, III, and IV, respectively. The solutions are for the invariant subspace with $r = N/2$ ($S_T^z = 0$) for even N or $r = (N-1)/2$ ($S_T^z = 1/2$) for odd N. For given momenta k_i, the phase angles θ_{ij} can be determined from (32) and the eigenvectors (27) by the substitution of k_i, θ_{ij} into (28). These solutions yield all the energy levels. Some of the levels are degenerate, namely those with one or several Bethe quantum numbers equal to zero. The remaining eigenvectors of any such level belong to the same S_T multiplet but have different r, i.e., different S_T^z. All Bethe ansatz solutions for $r < N/2$ (even N) or $r < (N-1)/2$ (odd N) can be inferred from the ones listed in Tables II, III, IV by removing the momenta $k_i = 0$ one at a time. Each $k_i = 0$ removed from a solution in the r subspace yields a solution in the $r+1$ subspace with the remaining k_i unchanged.

TABLE II. Bethe ansatz solutions for $N = 4$, $r = 2$.

S_T	$\lambda_1\lambda_2$	$2k/\pi$	k_1	k_2	$E - E_0$
2	0 0	0	0	0	0
1	0 1	1	0	$\pi/2$	1
1	0 2	2	0	π	2
1	0 3	3	0	$3\pi/2$	1
0	1 3	0	$2\pi/3$	$4\pi/3$	3
0	1 1	2	$\pi/2 + i\infty$	$\pi/2 - i\infty$	1

TABLE III. Bethe ansatz solutions for $N = 5$, $r = 2$.

S_T	$\lambda_1\lambda_2$	$5k/2\pi$	k_1	k_2	$E - E_0$
5/2	0 0	0	0	0	0
3/2	0 1	1	0	$2\pi/5$	0.690983
3/2	0 2	2	0	$4\pi/5$	1.809016
3/2	0 3	3	0	$6\pi/5$	1.809016
3/2	0 4	4	0	$8\pi/5$	0.690983
1/2	1 3	4	1.705325	3.321222	3.118033
1/2	1 4	0	$\pi/2$	$3\pi/2$	2
1/2	2 4	1	2.961962	4.577859	3.118033
1/2	1 1	2	$2\pi/5 + i1.198913$	$2\pi/5 - i1.198913$	0.881966
1/2	4 4	3	$8\pi/5 + i1.198913$	$8\pi/5 - i1.198913$	0.881966

For large N, the classification of the Bethe ansatz solutions becomes more and more intricate as r increases toward $N/2$, and finding them all becomes increasingly tedious. A more modest, but nevertheless highly promising and useful goal in many applications, is to find selected solutions for very large systems ($N \to \infty$) – solutions that determine specific physical properties (ground state energies, magnetization curves, susceptibilities, excitation spectra) of the underlying model system. This approach, to which many authors have made important contributions since 1931, will be explored in future columns.

We conclude with a brief discussion of some Bethe ansatz solutions for $r > 2$ that are of particular importance in the context of the Heisenberg ferromagnet ($J > 0$). Earlier we have found that two magnons may form a bound state with a considerable binding energy (see Fig. 2). We have seen that in these states the two down spins are much more likely to be on nearest-neighbor sites than is the case for two-magnon scattering states. The fact is that three or more magnons can form

TABLE IV. Bethe ansatz solutions for $N = 6$, $r = 3$.

S_T	$\lambda_1\lambda_2\lambda_3$	$3k/\pi$	k_1	k_2	k_3	$E - E_0$
3	0 0 0	0	0	0	0	0
2	0 0 1	1	0	0	$\pi/3$	1/2
2	0 0 2	2	0	0	$2\pi/3$	3/2
2	0 0 3	3	0	0	π	2
2	0 0 4	4	0	0	$4\pi/3$	3/2
2	0 0 5	5	0	0	$5\pi/3$	1/2
1	0 1 3	4	0	1.419506	2.769283	2.780775
1	0 1 4	5	0	1.340040	3.895947	5/2
1	0 1 5	0	0	$2\pi/5$	$8\pi/5$	1.381966
1	0 2 4	0	0	$4\pi/5$	$6\pi/5$	3.618033
1	0 2 5	1	0	2.387237	4.943144	5/2
1	0 3 5	2	0	3.513901	4.863679	2.780775
1	0 1 1	2	0	$\pi/3 + i0.732857$	$\pi/3 - i0.732857$	0.719223
1	0 5 5	4	0	$5\pi/3 + i0.732857$	$5\pi/3 - i0.732857$	0.719223
1	0 1 2	3	0	$\pi/2 + i\infty$	$\pi/2 - i\infty$	1
0	0 0 3	3	$i1.087070$	$-i1.087070$	π	0.697224
0	1 1 4	0	$\pi/2 + i\infty$	$\pi/2 - i\infty$	π	3
0	1 1 5	1	$1.338006 + i1.471688$	$1.338006 - i1.471688$	4.654369	2
0	1 5 5	5	1.628815	$4.945179 + i1.471688$	$4.945179 - i1.471688$	2
0	1 3 5	3	1.722768	π	4.560416	4.302775

bound spin complexes with even lower excitation energies. Specifically, for the subspace with r down spins, it can be shown that the lowest excited state at fixed wave number k is represented by the wave function with (complex) momenta given by

$$\cot\frac{k_j}{2} = r\cot\frac{k}{2} - i(r - 2j + 1) + O\big(e^{-\delta_j N}\big), \qquad (37)$$

with $\delta_j > 0$, $j = 1, \ldots, r$. This solution generalizes the case $r = 2$ discussed in Problem 9 and yields exact solutions for $N \to \infty$. The dispersion of the resulting bound state branch with $r \leq N/2$ is

$$E - E_0 = \frac{J}{r}(1 - \cos k). \qquad (38)$$

The Bethe quantum numbers of any such state are characterized by $|\lambda_i - \lambda_{i+1}| = 0, 1$ for every pair of complex conjugate momenta $k_{i+1} = k_i^*$ in (37).

In part II of this series, the focus will be on the 1D $s = 1/2$ Heisenberg antiferromagnet. We shall employ the Bethe ansatz to determine the ground state of this model, the spectrum of low lying excitations, and the calculation of transition rates for dynamical quantities.

Suggested problems for further study

1. The translation operator $\mathbf{T}$ shifts the local spin configuration to the left by one site with a wrap around at the ends, e.g., $\mathbf{T}|\uparrow\uparrow\downarrow\downarrow\rangle = |\uparrow\downarrow\downarrow\uparrow\rangle$. Show that the states (4) are eigenvectors of $\mathbf{T}$ with eigenvalues e^{ik} and eigenvectors of H with eigenvalues (5).

2. Each spin wave state contains one flipped spin. In a traveling wave it is located at each lattice site with equal probability. Show that the periodic nature of the disturbance in the spin alignment of a spin wave state is reflected in a $1/N$-correction of the spin correlation function:

$$\langle\psi|\mathbf{S}_l \cdot \mathbf{S}_{l+n}|\psi\rangle = \frac{1}{4} - \frac{2}{N}\sin^2\left(\frac{kn}{2}\right). \qquad (39)$$

   The nearest-neighbor correlation function defines an effective angle θ between nearest-neighbor spins: $\langle\psi|\mathbf{S}_l \cdot \mathbf{S}_{l+1}|\psi\rangle = \frac{1}{4}\cos\theta$. From (39) with $n = 1$ we see that the smaller the wavelength, the larger θ and the larger the energy (5) of the state. For $k = 0$ the spins remain fully aligned, and the state is degenerate with $|F\rangle$.

3. Show that the Bethe ansatz equations for $\lambda_1 = 0, \lambda_2 = 0, 1, \ldots, N - 1$ are solved by $k_1 = 0, k_2 = 2\pi\lambda_2/N, \theta = 0$. Use (14) instead of (16), which is singular in this case.

4. Express (19) for $k = 0$ in the form $\cot(Nk_1/2) = \cot(k_1/2)$, which yields $k_1 = -k_2 = 2l\pi/(N - 1)$ with integer l. For $k = \pi$, express (19) in the form $\cot(Nk_1/2) = \cot(k_1)$, which yields $k_1 = \pi - k_2 =$

$2l\pi/(N-2)$. For any such solution k_1, k_2 found, use (12) to determine the excitation energy and (16) and (17) to determine λ_1, λ_2.

5. Solving (19) is equivalent to finding the zeros of the function $f(x) = 2\cot(Nx) - \cot x + \cot(k/2 - x)$, where $x = k_1/2$. Standard subroutines such as can be found in Numerical Recipes[4] ask for an interval $[x_1, x_2]$ that contains exactly one zero of $f(x)$ such that $f(x_1) \gtrless 0, f(x_2) \lessgtr 0$. To fine tune this procedure, it is useful to preview the distribution of zeros by plotting $f(x)$ for $0 < x < \pi$ and various N.

6. Solving (21) is equivalent to finding the zero at $v > 0$ (if one exists) of the function $f(v) = \kappa \sinh(Nv) - \sinh([N-1]v) - \delta \sinh v$, where $\kappa = \cos(k/2)$, $\delta = 1$ for $\lambda_2 = \lambda_1$, and $\delta = -1$ for $\lambda_2 = \lambda_1 + 1$. Consider the case $\lambda_2 = \lambda_1$. Show that a zero of $f(v)$ exists if $N\kappa > 0$ and $N(\kappa - 1) < 0$, which implies (23). A similar argument yields the allowed Bethe quantum numbers for the case $\lambda_2 = \lambda_1 + 1$. Find the zero of $f(v)$ numerically for all allowed combinations of $\lambda_2 = \lambda_1$ and $\lambda_2 = \lambda_1 + 1$ and determine the energies via (22).

7. Insert (20) with $k = \pi, \phi = 0, \chi = vN$ into (15), and show that $a(n_1, n_2) = i(-1)^{n_1}\delta_{n_2, n_1+1}$ as $v \to \infty$. Show that these coefficients satisfy (11b) with $E - E_0 = J$. Show that the same coefficients result from the solution for $\lambda_1 = \lambda_2 = 3N/4$. This is the only $r = 2$ state whose Bethe quantum numbers are not unique.

8. Show that the operator $\mathbf{S}_T^2 = \left(\sum_{n=1}^N \mathbf{S}_n\right)^2$ commutes with H and S_T^z by using (2). Show that $\mathbf{S}_T^2|F\rangle = S_T(S_T+1)|F\rangle$ with $S_T = N/2$. Conservation of the total spin S_T implies that all eigenstates are at least $(2S_T + 1)$-fold degenerate. The level with energy E_0 has $S_T = N/2$, and hence its degeneracy is $N + 1$. It is represented in all r subspaces. For $r = 0$ it is the state $|F\rangle$, for $r = 1$ it is the one-magnon state with $k = 0$, and for $r = 2$ it is the class C_1 state with $k = 0$. The remaining one-magnon states in the $r = 1$ subspace have $S_T = N/2 - 1$, which implies an $(N - 1)$-fold degeneracy. They are represented in all r subspaces with $1 \le r \le N - 1$. For $r = 2$, they are the class C_1 states with $k \neq 0$. All other $r = 2$ states have $S_T = N/2 - 2$.

9. Show that for $N \to \infty$, the solution of $f(v) = 0$ with $f(v)$ as defined in Problem 6 converges toward $v(k) = -\ln\cos(k/2)$, which substituted into (22) yields (26). Show that $\cot k_{1,2}/2 = 2\cot k/2 \mp i$. For $k = \pi - 4\pi/N$, this solution is extremely accurate even for small N. Show that $|a(n_1, n_2)| \propto \cosh[(x - 1/2)N \ln N]$, where $0 < x = (n_2 - n_1)/N < 1$. Plot this distribution versus x for several N and with appropriate normalization. Demonstrate that all coefficients $a(n_1, n_2)$ with $n_2 - n_1 > 1$ go to zero as $N \to \infty$.

10. Show that Eqs. (16) and (17) for $\lambda_{1,2} = N/2 \mp 1$ are solved by $k_{1,2} = \pi[1 \mp 1/(N-1)]$ with $(E - E_0)/J = 4\sin^2 \pi/(N-1)$. This two-magnon scattering state is the highest $r = 2$ excitation energy. The wave function of this state has coefficients $a(n_1, n_2) = 2(-1)^{n_1+n_2}\sin[\pi(1/2 + n_1 - n_2)/(N-1)]$. Plot $|a(n_1, n_2)|$ versus $n_2 - n_1$ and compare this weight distribution with that of a two-magnon bound state.

ACKNOWLEDGMENTS

This work was supported by the U. S. National Science Foundation, Grant DMR-93-12252, and the Max Kade Foundation. We thank Scott Desjardins for his comments on the manuscript, Charles Kaufman for his help with the production of color figures, and the editors, Harvey Gould and Jan Tobochnik, for their helpful suggestions.

[1] W. Heisenberg, Z. Phys. **38**, 441 (1926); P. Dirac, Proc. Roy. Soc. London **112A**, 661 (1926).

[2] H. Bethe, Z. Phys. **71**, 205 (1931), *Zur Theorie der Metalle. Eigenwerte und Eigenfunktionen der linearen Atomkette.*

[3] G. H. Golub and C. F. van Loan, *Matrix Computations* (Johns Hopkins, Baltimore, 1993).

[4] W. H. Press, S. A. Teukolsky, W. T. Vetterling, and B. P. Flanner, *Numerical Recipes in C*, Cambridge University Press, Cambridge (1992).